Temperature response of aqueous solutions of pyrene end-labeled poly(N-isopropylacrylamide)s probed by steady-state and time-resolved fluorescence

Fowler, Michael

2018-02-15

Fowler , M , Duhamel , J , Qiu , X P , Korchagina , E & Winnik , F M 2018 , ' Temperature response of aqueous solutions of pyrene end-labeled poly(N-isopropylacrylamide)s probed by steady-state and time-resolved fluorescence ' , Journal of Polymer Science. Part B, Polymer Physics , vol. 56 , no. 4 , pp. 308-318 . https://doi.org/10.1002/polb.24543

http://hdl.handle.net/10138/308001
https://doi.org/10.1002/polb.24543

Temperature Response of Aqueous Solutions of Pyrene End-Labeled Poly(*N*-isopropylacrylamide)s Probed by Steady-State and Time-Resolved Fluorescence

Michael Fowler[a], Jean Duhamel*[a], Xing Ping Qiu[b], Evgenyia Korchagina[b], Françoise M. Winnik*[b,c,d]

a) Institute for Polymer Research, Waterloo Institute for Nanotechnology, Department of Chemistry, University of Waterloo, Waterloo, ON N2L 3G1, Canada

b) Department of Chemistry, Université de Montréal, CP 6128 Succursale Centre Ville, Montréal QC H3C 3J7, Canada

c) Department of Chemistry, and Faculty of Pharmacy, University of Helsinki, Helsinki, Finland

d) WPI Center for Materials Nanoarchitectonics (MANA), National Institute for Materials Science, (NIMS), 1-1 Namiki, Tsukuba 305-0044, Japan

Correspondence to: Jean Duhamel (E-mail: *jduhamel@uwaterloo.ca*)

((Additional Supporting Information may be found in the online version of this article.))

ABSTRACT

Aqueous solutions of a series of monodisperse poly(*N*-isopropylacrylamide)s end-labeled with n-butyl-1-pyrene at one or both chain ends (Py_n-PNIPAMs with n = 1 or 2) were studied by turbidimetry, light scattering, and fluorescence. For a given polymer concentration and heating rate, the cloud point (T_c) of an aqueous Py_n-PNIPAM solution, determined by turbidimetry, was found to increase with the number-average molecular weight (M_n) of the polymer. The steady-state fluorescence spectra and time-resolved fluorescence decays of Py_n-PNIPAM aqueous solutions were analyzed and all parameters retrieved from these analyses were found to be affected as the solution temperature passed through T_c, the solution cloud point, and T_m, the temperature where dehydration of PNIPAM occurred. The trends obtained by fluorescence to characterize the aqueous Py_n-PNIPAM solutions as a function of temperature were found to be consistent with the model proposed for telechelic PNIPAM by Koga et al. in 2006.

KEYWORDS: pyrene fluorescence, dynamic light scattering, poly(*N*-isopropylacrylamide), thermoresponsive, aggregation

INTRODUCTION

Aqueous solutions of poly(*N*-isopropylacrylamide) (PNIPAM) have been the subject of major scientific interest for over 50 years[1,2] and have been studied using a variety of techniques including viscometry,[3-5] turbidimetry,[4,6-9] light scattering,[5,9,10] fluorescence,[7,10-15] and neutron scattering.[16-19] The origin of this interest resides in the fact that PNIPAM possesses a lower critical solution temperature (LCST) in water. Its cloud point (T_c) is typically reported as 32 °C.[2,20-24] PNIPAM chains undergo a transition from soluble coils to dehydrated globules at T_c and these globules then form larger aggregates called mesoglobules.[20,25-28] The transition at T_c, also

referred to as the coil-to-globule transition (CGT), usually occurs over a narrow temperature range because the process of hydration/dehydration is cooperative.[29,30] The value of T_c for a given PNIPAM solution depends on a number of factors that include the polymer molecular weight and the polymer concentration,[9] if the solution is in the dilute regime. In the case of modified PNIPAM, the nature of the substituents and their distribution along the chain also affect T_c, particularly for polymers of $M_n < 50{,}000$ g mol^{-1}. The effect of the end-groups on T_c depends strongly on their polarity: [8,31-33] hydrophobic end-groups cause T_c to decrease, while hydrophilic end groups have the opposite effect.

Since the bridging induced by hydrophobic associations between hydrophobically modified water-soluble polymers such as Hydrophobically modified Ethoxylated Urethanes (HEURs), Hydrophobically Modified Alkali Swellable Emulsion copolymers (HASEs), or Hydrophobically Modified HydroxyEthyl Cellulose (HMHEC) often conveys industrially relevant viscoelastic properties to their aqueous solutions,[34,35] the modification of water-soluble PNIPAMs by covalent attachment of lipophilic groups (referred to as *lip*) bore the promise that temperature could be used as an additional parameter to further control the viscoelastic properties of aqueous solutions of *lip*-PNIPAMs. This realization led to a sustained scientific interest in understanding the complex interactions of *lip*-PNIPAMs that take place in water intra- and intermolecularly between the hydrophobic pendants and the PNIPAM backbone as a function of solution temperature. However the shear complexity of the different physical phenomena (hydrophobic associations, PNIPAM dehydration, macromolecular aggregation) occurring simultaneously in the aqueous solution led to the design of simpler *lip*-PNIPAM constructs such as telechelic monodisperse *lip*$_2$-PNIPAMs where two same hydrophobes were covalently attached to the ends of a monodisperse PNIPAM and the effects of these end-groups on the association mechanism have been investigated.[10,11,16-19,36,37] In essence such model compounds are the thermoresponsive equivalent of monodisperse HEURs and they are the focus of the present study. *lip*$_2$-PNIPAMs have been studied by light scattering, neutron scattering, fluorescence, and other techniques[10,11,16-19] and the results of these investigations have led to the establishment of a model describing the behaviour of aqueous solutions of *lip*$_2$-PNIPAM as the temperature increases. The key points of this model originally proposed for PNIPAM modified at both ends with n-octadecyl hydrophobes[10,16] have been depicted in Scheme 1 for *lip* = Py and are discussed hereafter.

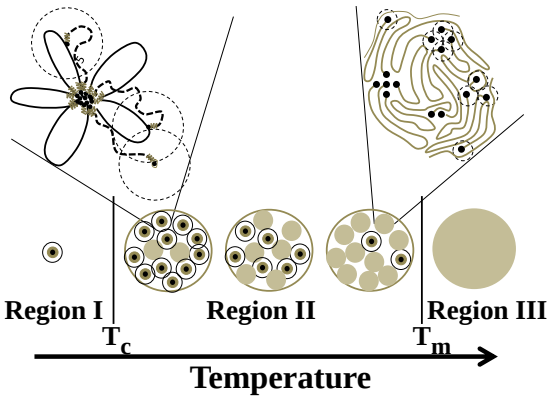

SCHEME 1 Effect of temperature on the distribution of the pyrene species and the morphology of the *lip*$_2$-PNIPAM chains. Color code: Black: pyrene; grey lines: dehydrated PNIPAM; black lines: solvated PNIPAM chains; dotted black lines: dangling PNIPAM chains.

Below 20 °C, *lip*$_2$-PNIPAM forms stable flower-like micelles with a three layered onion-like

structure. The innermost core is composed of the hydrophobes, the outermost shell is constituted of hydrated PNIPAM loops, and the middle region between the two consists of a mixture of water and dehydrated PNIPAM segments. As the temperature increases above 20 °C, the *lip*$_2$-PNIPAM solution enters the thermodynamic Regime I where segments of the PNIPAM loops in the shell begin to dehydrate and collapse into the middle region. Water is expelled from the middle region as the dehydrating chains of the shell collapse into it, leading to a constant volume for the middle region and a decrease in the volume of the shell.[18] As dehydrated PNIPAM chain segments also enter the hydrophobic core, the core becomes more hydrophilic.[10] This behaviour continues until T_c is reached.

At T_c, the *lip*$_2$-PNIPAM solution enters Regime II where the micelles begin to associate with one another to form partly dehydrated larger aggregates, called mesoglobules. The apparent M_n of PNIPAM mesoglobules increases significantly while the internal fluidity of the mesoglobules decreases.[10,14] As the temperature approaches the stable mesoglobule temperature of 34 °C (T_m),[10] the mesoglobules increase in size and the hydrophobic cores of the original micelles dissociate and disperse throughout the mesoglobule. At the same time, additional water is expelled from the mesoglobules.[14] Above T_m, the *lip*$_2$-PNIPAM solution enters Regime III where mesoglobules stabilize and do not grow any further. At this stage, the mesoglobules are thought to have an "almost frozen nature".[16,18] In all three regimes, any structures formed, either micelles or mesoglobules, do not interact with one another if the polymer concentration is below 1 g/L.[16,18,19] While the solutions of *lip*$_2$-PNIPAM show an M_n-dependence for T_c, T_m is always found to equal 34 °C regardless of M_n.

This description of the dehydration of *lip*$_2$-PNIPAM with increasing temperature suggests that the hydrophobes experience some rather drastic changes in their environment, as *lip*$_2$-PNIPAM incorporated in rosette micelles at low temperature transitions from isolated micelles in aqueous solution where the hydrophobes are somewhat exposed to the water phase, to aggregated micelles inside a mesoglobule at T_c where the hydrophobes are much more protected from the aqueous phase, to the dehydration of PNIPAM in Regime II which induces the dispersion of the hydrophobes throughout the dehydrated PNIPAM matrix and a reduction in their mobility. The phenomena described above can be investigated by studying the fluorescence response of a series of *lip*$_2$-PNIPAMs where the two hydrophobic ends were replaced by two pyrene chromophores to yield Py$_2$-PNIPAM constructs. Pyrene is ideally suited for such an investigation since it is hydrophobic and its fluorescence is sensitive to changes in its mobility and local concentration through pyrene excimer formation and its accessibility to the solvating medium through protective quenching.

To this end, a series of Py$_n$-PNIPAM samples (where *n* equals 1 or 2) were prepared with 1-pyrenebutyl groups to replace the octadecyl groups used in previous studies of *lip*$_2$-PNIPAM.[10,18,19,38] The behavior of the Py$_n$-PNIPAM samples was characterized not only by steady-state and time-resolved fluorescence, but also by turbidimetry and light scattering to establish the transition temperatures T_c and T_m. While turbidimetry and light scattering report on the behaviour of the entire polymer chain, fluorescence provides information on the

specific behaviour of the hydrophobes. The effect of temperature on the behavior of the pyrenyl groups was characterized as the temperature passed through T_c and T_m. The results obtained through this fluorescence study of the Py_n-PNIPAM samples established that the pyrenyl end groups responded to changes in solubility experienced by the macromolecule and the trends obtained from the fluorescence data appeared to fall within the framework describing the dehydration process of *lip*$_2$-PNIPAM.[10,16,18]

EXPERIMENTAL

Materials. Water was deionized with a Milli-Q UF Plus system (Bedford, MA) such that it had a resistivity exceeding 18 MΩ·cm. The pyrene-labeled PNIPAM samples were prepared by reversible addition fragmentation chain transfer polymerization (RAFT) of NIPAM followed by end-group modification with a pyrenylbutyl derivative. Their synthesis and characterization has been described in detail previously.[10,12,13] The degree of end-group substitution exceeded 75%. The number-average molecular weight (M_n) and polydispersity index of the samples are listed in Table 1. The following nomenclature was used to identify the samples: Py_1-PNIPAM refers to polymers singly-labeled with pyrene (or semi-telechelic), while Py_2-PNIPAM refers to the telechelic chains (see Figure 1). The number in brackets denotes the M_n of the PNIPAM backbone in kg/mol. The unlabeled PNIPAM sample of $20 < M_w < 25$ kg/mol (averaged to 22 kg/mol) was purchased from Sigma-Aldrich and used as received. Ethanol (HPLC grade reagent alcohol) was supplied by Fischer Scientific.

Solutions preparation. In order to avoid errors related to the hypochromicity of pyrenyl derivatives in water,[39] solutions of the polymers in ethanol were prepared first to determine the exact concentration of the Py_n-PNIPAM solutions, followed by solvent exchange from ethanol to water (see below). Solutions of the polymers in ethanol were prepared, starting from dry polymer powder. The polymer concentrations were determined from the UV absorbance at 344 nm of the pyrenylbutyl substituent, using the molar extinction coefficient ε_{Py} = 42,250 $mol^{-1}.L.cm^{-1}$ of 1-pyrenebutanol in ethanol. Subsequently, aliquots of the solutions were transferred in separate vials, in amounts calculated to yield, upon dilution, aqueous solutions having an absorbance at 344 nm of 0.1 ([pyrene] = 2.4 µmol L^{-1}). The ethanol was removed under a stream of nitrogen. Desired amounts of water were added to the residues. The mixtures were vortexed briefly and kept at 4 °C for at least 30 minutes prior to measurements. This protocol yielded Py_n-PNIPAM solutions of identical pyrene concentration ([pyrene] = 2.4 µmol.L^{-1}) and polymer concentrations ranging from 9.5 mg.L^{-1} to 59.0 mg.L^{-1} (Table 1). The unlabeled PNIPAM solution was prepared by dissolving a known weight of polymer in water to yield a 1 g.L^{-1} stock solution and reducing the concentration via successive dilutions to the desired polymer concentration.

Instrumentation and methods. The phase transition temperature of Py_n-PNIPAM aqueous solutions was determined by turbidimetry measurements performed on a Varian Cary 100 Bio UV-Vis spectrophotometer equipped with a 6×6 multicell sample holder thermostatted with a Peltier controller and able to cover a temperature range between –10 and 100 °C. The absorbance at 500 nm was recorded at 0.25 °C intervals as the temperature of aqueous Py_n-PNIPAM solutions (0.5 g.L^{-1}) was raised from 10 to 45 °C at a heating rate of 0.5 °C.min^{-1} .

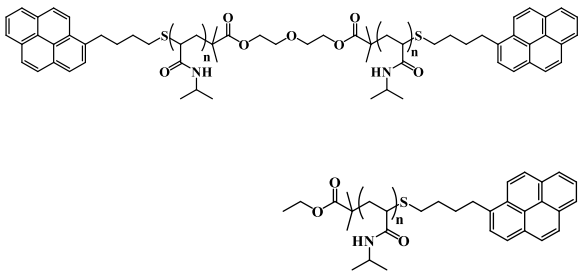

FIGURE 1 Chemical structure of (top) Py_2-PNIPAM and (bottom) Py_1-PNIPAM.

TABLE 1 Number-average molecular weight (M_n) and polydispersity index (PDI) of the PNIPAM samples and their concentrations for the fluorescence experiments.

Sample	M_n (kg/mol)	PDI	[Py_n-PNIPAM] (mg L^{-1})
Py_2-PNIPAM(7K)	7.6	1.08	9.5
Py_2-PNIPAM(14K)	13.7	1.10	17
Py_2-PNIPAM(25K)	25.4	1.07	32
Py_2-PNIPAM(45K)	44.5	1.10	56
Py_1-PNIPAM(7K)	7.68	1.02	18
Py_1-PNIPAM(12K)	12.3	1.02	30
Py_1-PNIPAM(25K)	23.5	1.09	59
PNIPAM(22K)	20-25		

Light scattering experiments were performed on an ALV GmbH instrument equipped with a CGS-3 goniometer and an ALV-5000 multiple digital time correlator. A He-Ne laser operating at a wavelength of λ_o = 632.8 nm was used as the light source. Before the measurements, all solvents and solutions were filtered through a 0.22 µm pore size filter. To confirm the transition temperatures obtained by turbidimetry, the phase transition temperature of aqueous Py_n-PNIPAM solutions (0.5 g.L^{-1}) was determined from the temperature-dependent scattering intensity measured at 90° of samples heated stepwise at an approximate rate of 0.5 °C.min^{-1}. Dynamic light scattering measurements were conducted with aqueous Py_n-PNIPAM solutions kept at 15 or 35 °C. The concentrations were adjusted to account for the difference in scattering intensity of solutions kept at 15 °C (low intensity) and at 35 °C (high intensity). The phase transition temperature of dilute Py_n-PNIPAM solutions used for measurements with polymer concentrations ranging between 10 and 60 mg.L^{-1} was determined using the steady-state fluorometer. Solutions were irradiated at 500 nm in the fluorometer. The intensity of the scattered light from 490 to 510 nm was determined in 0.5 nm increments as a function of temperature for samples heated from 20 to 40 °C at a rate equivalent to 0.1 °C.min^{-1} with 1 °C increments.

Steady-state fluorescence measurements were conducted using a Photon Technology International LS-100 steady-state fluorometer equipped with a continuous xenon lamp. Quartz fluorescence cells (VWR) with an inner cross section of 10 × 10 mm^2 were used and measurements were performed with a right angle geometry. They were placed in a temperature-controlled cell holder thermostated by an external circulating water bath. Pyrene fluorescence spectra were acquired upon excitation at 342 nm. The excitation and emission slits were set at 2.0 and 1.0 nm, respectively. For each temperature setting, the spectra acquisition took about 1 minute. The temperature was increased in 1.0 °C increments. Samples were allowed to equilibrate for 10 min after each temperature change. Thus, the fluorescence experiments were conducted with an average heating rate of about 0.1 °C.min^{-1} and with aerated solutions.

The fluorescence decay profiles were obtained with a time-correlated single photon counter

manufactured by IBH Ltd. using a NanoLED 340 nm diode as the excitation source. Samples were excited at 342 nm, and the emission wavelength was set at 375 nm and 510 nm for the pyrene monomer and excimer, respectively. The samples were placed in a 10 × 10 mm^2 fluorescence cell (VWR) and left to equilibrate at the set temperature for 10 minutes. Monomer and excimer decays acquisition took about 5 minutes before the temperature was raised by 1 °C to repeat the process. Thus the heating rate of the time-resolved fluorescence experiments can be estimated to equal 0.07 °C.min^{-1}. All decays were collected with the right angle geometry over 1,024 channels with a minimum of 20,000 counts taken at the decay maximum to ensure a high signal-to-noise ratio. A light scattering standard was used to determine the instrument response function (IRF).

Data analysis. The transmission-vs-temperature profile used to monitor the turbidity of the Py_n-PNIPAM aqueous solutions such as shown in Figures 1A or S1 in Supporting Information (SI) were analyzed as follows. The derivative of the transmittance with respect to temperature was determined, and T_c was taken as the point of intersection between the baseline and the rise in the derivative. An example of the determination of T_c by turbidimetry may be found in Figure S1.

A light scattering correction was applied to the analysis of the fluorescence spectra by subtracting the spectrum obtained from the light scattered by a non-fluorescently labeled PNIPAM(22K) solution at the same polymer concentration, scaled for intensity, from the fluorescence spectrum of the Py_n-PNIPAM solution. Since the excimer fluorescence maximum of the Py_2-PNIPAM samples was found to shift with increasing temperatures at temperatures above T_c, the excimer emission was extracted as follows (see Figure S3 in SI). The fluorescence spectrum of the Py_1-PNIPAM(25K) sample was used as monomer spectrum since it showed hardly any excimer emission. The spectrum of Py_1-PNIPAM(25K) at the desired temperature was normalized to the band at 375 nm of a Py_2-PNIPAM fluorescence spectrum. The normalized Py_1-PNIPAM(25K) spectrum was subtracted from the Py_2-PNIPAM spectrum to yield the excimer fluorescence spectrum. The normalized monomer fluorescence spectra of Py_1-PNIPAM(25K) were integrated across their entire wavelength range and the excimer spectra were integrated from 420 to 600 nm to yield I_M and I_E, respectively. The I_M and I_E values were used to calculate the I_E/I_M ratio. The isolated excimer fluorescence spectrum was fitted with a polynomial between 435 and 535 nm to determine the wavelength (λ_{max}) of the fluorescence intensity maximum. Since no shift in excimer fluorescence was observed for the Py_1-PNIPAM samples, the I_M and I_E fluorescence intensities were calculated by taking the integral under the fluorescence signal from 372 to 378 nm and from 500 to 530 nm, respectively.

Analysis of the fluorescence decays was performed with a sum of typically three exponentials as shown in Eq. 1. To ensure the reproducibility of the fluorescence decay analysis, decays were acquired in triplicate.

$$i(t) = \sum_{i=1}^{3} a_i \exp(-t/\tau_i) \qquad (1)$$

The pre-exponential factors and decay times used in Eq. 1 were optimized using the Marquardt–Levenberg algorithm.[40] The quality of the fits was established from the χ^2 values

(<1.30) and the random distribution around zero of the residuals and of the autocorrelation function of the residuals.

The number-average ($<\tau>_M$) lifetimes of the pyrene monomer fluorescence decays were calculated using Eq. 2.

$$<\tau>_M = \frac{\sum a_i \tau_i}{\sum a_i} \qquad (2)$$

The parameters a_i and τ_i referred to, respectively, the i^{th} pre-exponential factor and decay time obtained from the multi-exponential fit of the decays with Eq. 1. The number-average lifetime of the excimer $<\tau>_E$ was also obtained by applying Eq. 2 to those decay times with positive pre-exponential factors. Representative pyrene monomer fluorescence decays and the corresponding fluorescence spectra are shown in Figures S4A and S4B, respectively.

RESULTS AND DISCUSSION

Solution properties of Py_n-PNIPAM in water, a brief overview.

Dynamic light scattering measurements performed on aqueous Py_n-PNIPAM solutions kept at 15 °C indicated that the polymers self-assembled in water, forming particles of hydrodynamic radii (R_h) on the order of 4 to 9 nm, depending on the polymer molar mass and degree of labeling (Table 2). For telechelic polymers, the R_h values increased with increasing molar mass, as observed also in the case of α,ω-dioctadecyl-PNIPAM samples studied previously.[10] However, the Py_2-PNIPAM particles were smaller than their $(C_{18})_2$ counterparts, an indication of hydrophobe-induced differences in chain packing within the particles core. The longest polymers among the semi-telechelic samples investigated here, namely Py_1-PNIPAM(25K) and Py_1-PNIPAM(12K), were molecularly dissolved in water (15 °C, 0.5 g L^{-1}) since their measured R_h value matched within experimental error their theoretical R_h value. In contrast, Py_1-PNIPAM(7K), which features h a lower hydrophilic-to-lipophilic balance (HLB) value, formed rosette micelles with a pyrene-rich core stabilized by the PNIPAM chains in water at 15 °C since its measured R_h value was substantially larger than the R_h value for an individual chain.

The Py_n-PNIPAM solutions showed a marked sensitivity to temperature: their transmittance decreased sharply (Figure 2A) as the temperature exceeded a temperature (T_c), ranging from 16 °C to 31 °C, depending on polymer structure (telechelic-vs-semi-telechelic) and molecular weight. T_c increased with increasing M_n (Figure 2B), as a consequence of the increase in NIPAM units per pyrene groups associated with the increase in M_n. The trends observed in Figure 2 are consistent with previous studies.[8,10]

The temperature-driven enhancement of the intensity of light scattered by the solutions (Figure S5) reflects the formation of larger particles. The R_h values of the particles formed at 35 °C were ~ 100 nm (Table 2), a value typical of PNIPAM mesoglobules formed in dilute solution upon dehydration, collapse, and aggregation of PNIPAM chains when heated past their solution cloud point.[16] The R_h values recorded for Py_n-PNIPAM solutions were significantly larger than those of particles obtained previously with $(C_{18})_2$-PNIPAM solutions at 35 °C (Table 2), although in cold water the particles formed by Py_2-PNIPAM are smaller than those formed by $(C18)_2$-PNIPAM. The weaker aggregation of the pyrene groups of the Py_2-PNIPAM samples, compared to the C_{18} groups of the $(C_{18})_2$-PNIPAM samples, must

have resulted in more dangling pyrene pendants (See Scheme 1) in the corona of the rosette micelles. These groups provide sticky patches to facilitate adhesion of a larger number of rosette micelles at T_c, thus generating larger Py_2-PNIPAM mesoglobules.

TABLE 2 Hydrodynamic radii of *lip*$_n$-PNIPAM samples determined by DLS below T_c (15 °C or 20 °C) and above T_c (35 °C) where *lip* is either a 1-pyrenebutyl or octadecyl hydrophobe.

Samples	Mw$^{\Delta}$, kDa	$R_h(C_{18})$,[a] nm (20 °C)	$R_h(C_{18})$,[b] nm (35 °C)	R_h(Py),[c] nm (15 °C)	R_h(Py),[d]nm (35 °C)	R_h(Py), nm theoretical
Py_2-PNIPAM	7			5.0±0.2		2.5
	14	10.8	25	5.9±0.4	65	3.6
	25	12.9	28	8.1±0.5	85	4.8
	45	17.5	39	8.9±0.5	100	6.5
Py_1-PNIPAM	7			6.4±0.4		2.5
	12			4.0±1.0		3.3
	25			4.9±0.5		4.8

$^{\Delta}$ M_w provided for $(Py)_2$-PNIPAM (analogous masses for $(C_{18})_2$-PNIPAM are 12, 22, and 49 kDa, respectively); [a]@ 20 °C and concentration 1 g/L (Values taken from ref. 10); [b]@ 35 °C and concentration 0.3 g/L; [c]@ 15 °C and concentration 2 g/L; [d]@ 35°C and concentration 0.017, 0.03 and 0.06 g/L for 14, 25 and 45 kDa samples, respectively. Lower Lip$_n$-PNIPAM concentrations were used at $T > T_c$.

As shown in Figures S6A and B, the polymer concentration affects T_c substantially, a lower polymer concentration resulting in a higher T_c value. Consequently, turbidity experiments were unable to predict what the T_c value would be for the much more dilute Py$_n$-PNIPAM solutions used in the fluorescence experiment (see Table 1 for polymer concentrations).

The T_c values of the solutions used for the fluorescence experiments were obtained by monitoring the changes with temperature of the scattered light intensity from the Py$_n$-PNIPAM aqueous solutions placed in the sample compartment of the steady-state fluorimeter. The right-angle geometry was used and the scattered light was monitored at 500 nm, a wavelength where pyrene does not absorb light (Figure 3). The LS intensity increased sharply as the temperature reached a given value, taken as the T_c value as done in a previous publication.[38]

T_c was found to equal 22, 24, 28, and 28 °C in Figure 3A for Py_2-PNIPAM(7K), Py_2-PNIPAM(14K), Py_2-PNIPAM(25K), and Py_2-PNIPAM(45K), respectively. The T_c values increased with increasing molecular weight, as noted above. However the increase was not directly proportional to M_n as was observed by turbidimetry and DLS in Figure 2B for a 0.5 g.L^{-1} polymer concentration.

The LS intensity for the semi-telechelic samples, presented in Figure 3B, showed a sharp increase at 30 °C for all three samples. Based on the trends obtained by light scattering, the transition at 30 °C was assigned to T_c in good agreement with the turbidimetry results presented in Figure S6A that showed that T_c for the semi-telechelic samples seemed to cluster around 30 °C as the polymer concentration decreased.

While the turbidimetry measurements indicated that the hydrophobic pyrenes played a role in the dehydration of the Py$_n$-PNIPAM samples, they did not describe how dehydration of the PNIPAM chains affected the hydrophobes. This information was readily accessible from the analysis of the fluorescence spectra and decays of the Py$_n$-PNIPAM solutions

that report directly on the state of the pyrene labels.[41,42]

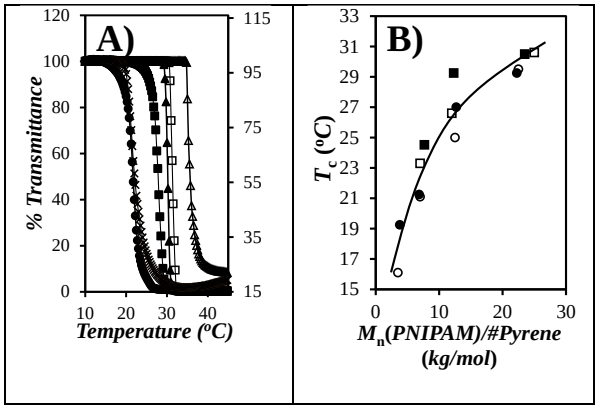

FIGURE 2 Turbidimetry measurements for 0.5 g/L pyrene-labeled PNIPAM samples with a heating rate of 0.5 °C/min. A) (×) Py_2-PNIPAM(7K), (●) Py_2-PNIPAM(14K), (■) Py_2-PNIPAM(25K), (▲) Py_2-PNIPAM(45K), (□) Py_1-PNIPAM(25K), and (Δ) PNIPAM(22K). B) T_c as a function of the ratio of M_n for the Py_n-PNIPAM samples over their respective number of pyrenes. (●) Py_2-PNIPAM and (■) Py_1-PNIPAM for T_c by turbidimetry, (○) Py_2-PNIPAM, and (□) Py_1-PNIPAM for T_c by DLS. Solid line is drawn to guide the eye.

In order to facilitate comparison between the spectra of the various samples, all solutions had the same pyrene concentration of 2.4 µM. As shown in Table 1, the polymer concentration of the solutions ranged from 9.5 mg.L^{-1} for Py_2-PNIPAM(7K) to 56 mg.L^{-1} for Py_2-PNIPAM(45K) as the longer chains required a larger massic concentration to achieve a same pyrene concentration as the shorter chains. These concentrations are significantly lower than the concentration (500 mg L^{-1}) of the Py_2-PNIPAM solutions used for turbidity assays (see Figure 2). The fluorescence experiments are now described in detail.

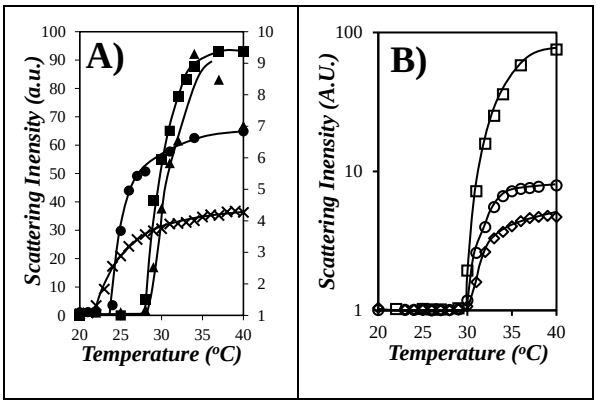

FIGURE 3 Normalized light scattering intensity of Py_2-PNIPAM samples as a function of temperature, Abs(342nm) = 0.1. A) (×, right axis) Py_2-PNIPAM(7K), (●, left axis) Py_2-PNIPAM(14K), (■, right axis) Py_2-PNIPAM(25K), and (▲, left axis) Py_2-PNIPAM(45K). B) (◇) Py_1-PNIPAM(7K), (○) Py_1-PNIPAM(12K), and (□) Py_1-PNIPAM(25K). Polymer concentrations are listed in Table 1.

Fluorescence study of aqueous solutions of the telechelic Py_n-PNIPAM samples: Steady state measurements. The emission spectra recorded for the Py_2-PNIPAM(14K) solution heated from 15 to 40 °C are presented in Figure 4. They are normalized to the intensity of the I_1 peak of the pyrene monomer at 375 nm. The intensity of the excimer emission at about 475 nm increases with increasing temperature up to T_c, at which point the excimer intensity decreases and its wavelength maximum undergoes a blue shift. Changes in the relative excimer intensity reflect changes in the interactions between the hydrophobic pyrene groups. Since steady-state fluorescence of pyrene reports directly on the behavior of the hydrophobic groups within a Py_2-PNIPAM polymer, the relationship between temperature and excimer fluorescence intensity was further investigated by the determination of the ratio of the fluorescence intensity of the excimer over that of the monomer, namely the I_E/I_M ratio.

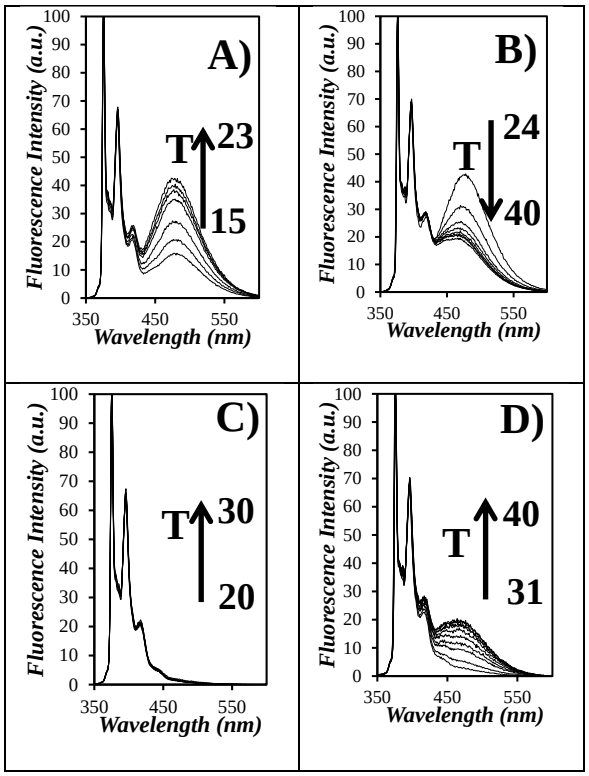

FIGURE 4 Steady-state fluorescence spectra for Py_2-PNIPAM(14K) for A) *T* increases from 15 to 23 °C and B) T increases from 24 to 40 °C, and Py_1-PNIPAM(7K) for C) *T* increases from 20 to 30 °C and D) *T* increases from 31 to 40 °C. Polymer concentrations are listed in Table 1.

The position of the excimer fluorescence maximum (λ_{max}) was also determined. Changes with increasing temperature of I_E/I_M and λ_{max} are shown in, respectively, Figures 5A and B for all the Py_2-PNIPAM samples.

For each Py_2-PNIPAM sample the maximum value in I_E/I_M corresponds to the temperature where the sharp increase in light scattering intensity was recorded (Figure 3). The increase in I_E/I_M for temperatures lower than T_c reflects an increase in the local pyrene concentration $[Py]_{loc}$ possibly caused by the contraction of the polymer coils within the micelles. Although the coil size might decrease while I_E/I_M increases with increasing temperature in Regime I, no significant increase in light scattering intensity took place over this temperature range (see Figure 3), indicating that the individual micelles did not assemble into objects large enough to scatter light. Following this increase, I_E/I_M reached a maximum at or near T_c before beginning to decrease with increasing temperature. The origin of the decrease in I_E/I_M above T_c could be inferred from the observation that the excimer emission maximum concommitantly shifts to shorter wavelengths. The plot of the wavelength at the maximum fluorescence intensity of the excimer (λ_{max}) as a function of temperature in Figure 5B confirmed that λ_{max} began to decrease at T_c, a temperature regime corresponding to Region II. The blue shift in the excimer emission wavelength has been assigned to a higher energy excimer species with partial overlap of the pyrenyl moieties.[43,44] The blue shift took place after the polymer underwent its cloud point transition and entered Regime II. The temperature-driven decrease in I_E/I_M and the concurrent shift in λ_{max} were most pronounced in the case of the shortest polymer, as observed in Figures 5A and B where we present individual plots recorded for each sample. The changes were hardly detectable for Py_2-PNIPAM(45K), due to the very low amount of excimer obtained with this sample and it was not possible to estimate reliably the shift in λ_{max} for this sample.

Since the behavior of the Py_n-PNIPAM samples depends on their HLB, the fluorescence spectra of Py_2-PNIPAM(14K) in Figures 4A and B were compared to those of Py_1-PNIPAM(7K) in Figures 4C and D. At low temperature, the semi-telechelic sample spectrum shows no excimer, indicating that the polymer iss not aggregated at the low (17 mg/L) concentration used for the fluorescence measurements. At 30 °C, which corresponds to T_C, aggregation takes place, resulting in Py excimer formation (Figure 4D).

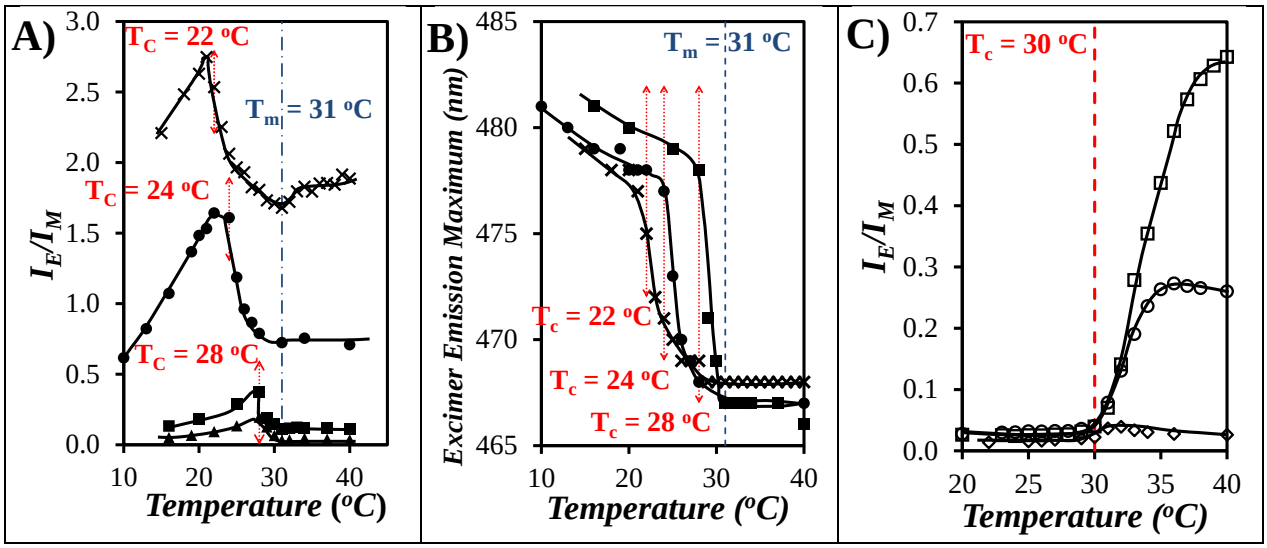

FIGURE 5 A) I_E/I_M ratio and B) wavelength at the excimer intensity maximum, for the Py_2-PNIPAM samples in water as a function of temperature. (×) Py_2-PNIPAM(7K), (●) Py_2-PNIPAM(14K), (■) Py_2-PNIPAM(25K), and (▲) Py_2-PNIPAM(45K). C) I_E/I_M ratio for (◇) Py_1-PNIPAM(7K), (○) Py_1-PNIPAM(12K), and (□) Py_1-PNIPAM(25K). Polymer concentrations are given in Table 1.

The changes observed in the fluorescence spectra acquired with the Py_nPNIPAM samples indicated that the fluorescence of the pyrene labels reflected the changes that were happening to the polymer as the solution temperature passed through T_c and T_m. More information about the state of the pyrene labels could be obtained through the analysis of their fluorescence decays as described hereafter.

Fluorescence study of aqueous solutions of the telechelic Py_n-PNIPAM samples: Time-resolved measurements. Time-resolved fluorescence decays of the pyrene monomer and excimer emissions of Py_2-PNIPAM aqueous solutions were acquired as a function of temperature. For all Py_2-PNIPAM samples, the decays were analyzed by performing a tri-exponential fit with Eq. 1. The number-average lifetime, $<\tau>_M$, of the pyrene monomer decay is plotted as a function of temperature in Figure 6A.

At temperatures lower than T_c, $<\tau>_M$ decreased slightly with temperature for all Py_2-PNIPAM samples. This decrease in $<\tau>_M$ for T < T_c might be related to the concomitant increase in excimer emission in this temperature range (see Figure 5A) Above T_c, $<\tau>_M$ increased with increasing temperature up to a temperature of ~32-33 °C, which corresponds to the end of Regime II marked by T_m. The $<\tau>_M$ of Py_2-PNIPAM(7K) remained more or less constant throughout the temperature domain probed. From 16 °C to T_c, the I_E/I_M ratio in Figure 5A increased by 25, 53, 190, and 300% for the Py_2-PNIPAM samples with M_n equal to 7, 14, 25, and 45K, respectively. Since the change in I_E/I_M was smallest for the Py_2-PNIPAM(7K) sample, minor changes in $<\tau>_M$, that should normally reflect a change in I_E/I_M, could not be assessed reliably, resulting in the almost flat $<\tau>_M$-vs-T profile for the shorter polymer in Figure 6A. The decrease in $<\tau>_M$ observed for the higher molecular weight Py_2-PNIPAM samples (M_n = 12, 25, and 45K) as the temperature increased toward T_c might be reasonably explained by a substantial increase in the amount of excimer being formed as observed in Figure 5.

Above T_c, the monomer lifetime increased significantly due to the collapse of the dehydrated PNIPAM chains which induced a decrease in the quenching efficiency of oxygen, a decrease in the rate of excimer formation by diffusion due to decreased local mobility, or both effects combined. In case of the longer Py_2-PNIPAM(45K) sample, the increase in $<\tau>_M$ is most likely due to a reduction in oxygen quenching efficiency, since the excimer emission was very weak for this sample. All these results agree well with the steady-state fluorescence data, showing a maximum level of excimer formation around T_c and a continuous decrease in excimer formation by diffusion due to the reduced mobility of the PNIPAM chains as they dehydrate throughout Regime II up to a temperature T_m of ~31-33 °C, depending on sample and type of experiment.

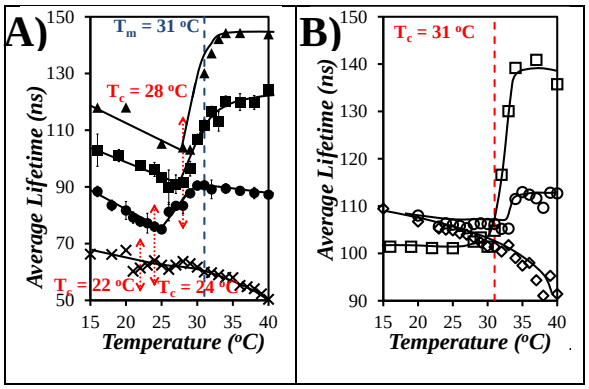

FIGURE 6 Number-average lifetime of the pyrene monomer decays for A) the Py_2-PNIPAM and B) the Py_1-PNIPAM samples in water as a function of temperature. (×) Py_2-PNIPAM(7K), (●) Py_2-PNIPAM(14K), (■) Py_2-PNIPAM(25K), (▲) Py_2-PNIPAM(45K), (◇) Py_1-PNIPAM(7K), (○) Py_1-PNIPAM(12K), and (□) Py_1-PNIPAM(25K) Polymer concentrations are listed in Table 1. Vertical arrows indicate T_c and T_m values.

Having accounted for the trends obtained from the analysis of the monomer decays of the Py_2-PNIPAM samples, we now focus on the analysis of their excimer decays. Multi-exponential fits of the excimer decays were performed. The average lifetime of the excimer $<\tau>_E$ and the ratio a_{E-}/a_{E+} were plotted as a function of solution temperature in Figure 7. The ratio a_{E-}/a_{E+}, equal to the sum of the negative pre-exponential factors over the sum of the positive pre-exponential factors and retrieved from the fit of the excimer decay with Eq. 1, is a measure of the amount of excimer formed by diffusion. A value of 0 for a_{E-}/a_{E+} indicates full aggregation while a value of −1 indicates purely diffusion-controlled excimer formation.[39,42] For solution temperatures below T_c, $<\tau>_E$ = 65 ± 2 ns. The $<\tau>_E$ values for Py_2-PNIPAM (Figure 7A) increased significantly around the T_c of the samples. As with the monomer decays, $<\tau>_E$ increased at temperatures above T_c due to the decrease in oxygen quenching and the slower diffusion of pyrene that led to less excimer formation. The increase in $<\tau>_E$ continued up to T_m = 32 °C for all Py_2-PNIPAM samples except Py_2-PNIPAM(7K). For this sample, strong pyrene aggregation and the poor protection against oxygen quenching by the much shorter PNIPAM chain probably accounted for the weak changes of the pyrene lifetimes. The ratio a_{E-}/a_{E+} took a negative value just before T_c that was equal to −0.10, −0.32, −0.35, and −0.36 for, respectively, the 7, 14, 25, and 45K Py_2-PNIPAM samples. The more negative ratios obtained for the longer constructs indicate that the longer chains result in a larger molar fraction of pyrene labels forming excimer by diffusion, albeit at a much slower rate. The a_{E-}/a_{E+} ratio became less negative at T_c due to an increase in the molar fraction of aggregated pyrenes and a decrease in excimer formation by diffusion due to the reduced mobility experienced by the PNIPAM backbone above T_c. These changes in the behaviour of a_{E-}/a_{E+} started at T_c and ended at a temperature of ~32 °C which was attributed to T_m marking the end of Regime II.

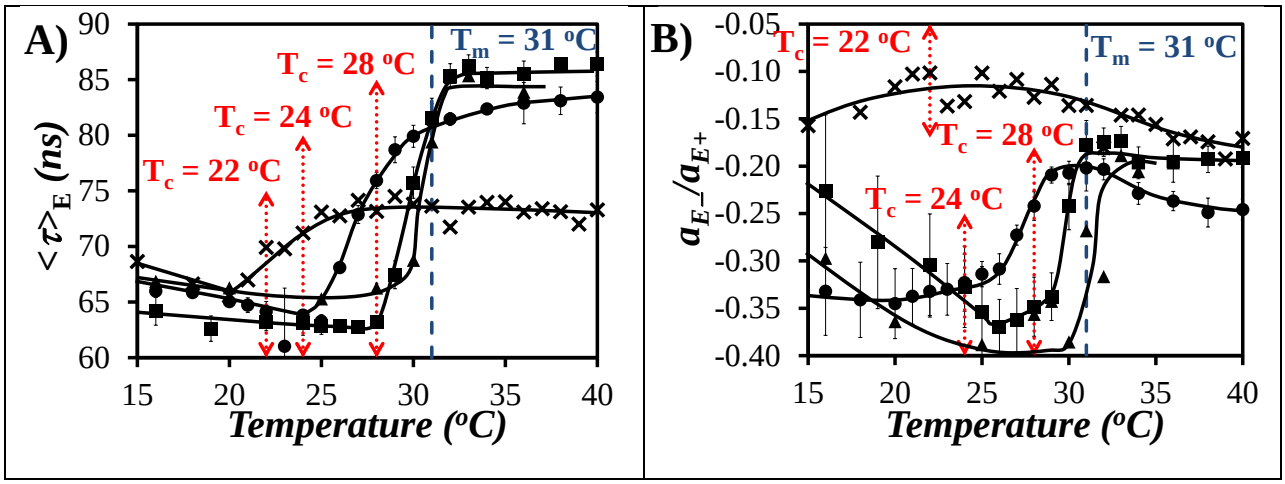

FIGURE 7 A) $\langle\tau_N\rangle_E$ obtained with decay times having positive pre-exponential factors and B) a_{E-}/a_{E+} ratio as a function of solution temperature. (×) Py_2-PNIPAM(7K), (●) Py_2-PNIPAM(14K), (■) Py_2-PNIPAM(25K), and (▲) Py_2-PNIPAM(45K)

The large error bars observed for Py_2-PNIPAM(25K) below T_c reflected large variations in a_{E-}/a_{E+} for decays obtained in this temperature range. The lack of a clear transition in a_{E-}/a_{E+} for the Py_2-PNIPAM(7K) sample was likely due to the more positive value of a_{E-}/a_{E+} below T_c (= 22 °C), which is approximately equal to the value of a_{E-}/a_{E+} above T_c, a consequence of the strong level of pyrene aggregation experienced by this sample.

The fluorescence decays of the pyrene monomers of the semi-telechelic samples were also acquired and analyzed to yield their $\langle\tau\rangle_M$ values which are plotted as a function of temperature in Figure 6B. The $\langle\tau\rangle_M$ behavior of the Py_1-PNIPAM(12K) and Py_1-PNIPAM(25K) samples closely resembled that of the Py_2-PNIPAM samples, increasing at T_c (=31 °C) and plateauing above T_m while the Py_1-PNIPAM(7K) showed no clear transition at T_c. As for the Py_2-PNIPAM samples, the increase of $\langle\tau\rangle_M$ at T_c was attributed to lower quenching from oxygen dissolved in water.

Differences between the behavior of the Py_1-PNIPAM and Py_2-PNIPAM samples. The trends observed with the Py_1-PNIPAM samples exhibited some features that were similar to those obtained with the Py_2-PNIPAM samples. In particular, the light scattering intensity, I_E/I_M, and $\langle\tau\rangle_M$ showed a pronounced change at T_c. There were however significant differences between the two families of Py_n-PNIPAM samples. The Py_1-PNIPAM samples did not show any M_n-dependence with regard to T_c as determined by light scattering, I_E/I_M, or $\langle\tau\rangle_M$. $\langle\tau\rangle_M$ remained constant with temperature in Regime I, and I_E/I_M did not pass through a maximum at T_c but instead, began to increase with increasing temperature once T_c was reached for the Py_1-PNIPAM(12K) and Py_1-PNIPAM(25K) samples.

The differences in behavior for $\langle\tau\rangle_M$ and I_E/I_M between the Py_1-PNIPAM samples and their corresponding Py_2-PNIPAM samples were best explained by the fact that Py_1-PNIPAM formed significantly less excimer than Py_2-PNIPAM, a consequence of the inability of the semi-

telechelic samples to form micelles below T_c as confirmed by the R_H values of the 12 and 25K Py_1-PNIPAM constructs measured by DLS which matched the predicted values for isolated coils in Table 2. The difference between measured and predicted R_h values for Py_1-PNIPAM(7K) in Table 2 suggests that this sample forms polymeric aggregates at the concentration of 2 $g.L^{-1}$ used in the DLS experiments. However the absence of excimer fluorescence in Figure 5C indicates that no Py_1-PNIPAM(7K) aggregates form at the much lower concentration of 17 $mg.L^{-1}$ used in the fluorescence experiments, certainly a consequence of the much lower polymer concentration. As the temperature increased in Regime I, $<\tau>_M$ and I_E/I_M for Py_1-PNIPAM remained constant because each chain contained only one pyrene. Thus a decrease in the radius of gyration of the chains did not change the local pyrene concentration and had no effect on pyrene excimer formation for these singly labeled chains. When mesoglobules formed in Regime II, the significant reduction in the mobility of pyrene did not result in a decrease in I_E/I_M as was observed for the Py_2-PNIPAM polymers in Figure 5A since very little diffusional excimer was present before the transition which could be affected by this change. Instead, the aggregation of chains into larger particles actually increased the local pyrene concentration and allowed more excimer to form for the Py_1-PNIPAM samples.

Agreement between fluorescence data and Scheme 1: The light scattering and fluorescence trends observed thus far are best explained using the model describing the dehydration of *lip*$_2$-PNIPAM in aqueous solution (see Scheme 1).[10,16,19] In Regime I, the Py_2-PNIPAM chains in solution are primarily found in polymeric micelles or single chains. These solutions exhibit low light scattering intensity due to the small size of the micelles and chains. The hydrophobic pyrenes are relatively exposed to the solution resulting in shorter monomer and excimer lifetimes due to greater exposure to oxygen dissolved in the aqueous phase. As the temperature increases in Regime I, the size of the micelles decreases which increases the local pyrene concentration, resulting in an increase in I_E/I_M and a slight decrease in $<\tau>_M$.

At T_c, the solutions enter Regime II which results in the formation of mesoglobules. The resulting increase in particle size, observed by DLS, causes an increase in both the turbidity and light scattering signals. The larger particles are better able to protect pyrene from quenching by oxygen in the solution, causing an increase in $<\tau>_M$ and $<\tau>_E$. The more hindered diffusion within the dehydrated mesoglobules reduces the mobility of the pyrene labels, reducing their ability to form excimer by diffusion; this causes a blue-shift in the wavelength of maximum excimer emission, a decrease in I_E/I_M, and an increase in the a_{E-}/a_{E+} ratio. The changes that occur at T_c for these parameters continue into Regime II, until they plateau at or before T_m. Above T_m in Regime III, all parameters remain constant. These observed trends for the light scattering and fluorescence parameters are consistent with the predictions made by the existing model describing the behavior of *lip*$_2$-PNIPAM samples in aqueous solution as a function of temperature.[10,16,19]

CONCLUSIONS

The use of fluorescence to probe the behaviour of aqueous solutions of pyrene end-labeled PNIPAMs has demonstrated that the behaviour of the hydrophobic pyrene labels is intimately linked to that of the polymeric constructs as

similar transitions were observed by LS which probes the entire polymer and fluorescence that only probes the end groups. Turbidimetry and light scattering have shown that the value of T_c depends on the hydrophobe content of the telechelic polymers, which is consistent with earlier work.[8] Analysis of the steady-state fluorescence spectra and the time-resolved fluorescence decays yielded a set of parameters indicating that the pyrene labels responded to changes in polymer conformations induced by changes in solution temperature as the solution temperature increased past a T_c value that depended on PNIPAM chain length and a T_m value that seemed little affected by PNIPAM chain length. Most importantly, the behavior of the pyrenyl groups probed by fluorescence agreed very well with expectations based on the model presented in Scheme 1.

The Py_1-PNIPAM samples showed significant behavioral changes at T_c. Even though the change in behaviour was different from that observed with the Py_2-PNIPAM samples, these differences could be traced back to the differences in the ability of telechelic and semi-telechelic PNIPAM to form pyrene excimer. All light scattering and fluorescence results were largely consistent with the accepted model representing the dehydration of *lip*$_2$-PNIPAM in aqueous solution.[10,16-19] Specifically, the decrease in micellar size in Regime I and the formation of mesoglobules in Regime II have been confirmed via light scattering, steady-state, and time-resolved fluorescence measurements.

Finally, the fact that the dehydration of the Py_n-PNIPAM samples could be observed by light scattering that probes the entire polymer coil and pyrene fluorescence that probes the hydrophobic end groups only is quite remarkable since the dehydration of the Py_n-PNIPAM samples is believed to start with the PNIPAM segments located close to the hydrophobic end groups. This observation demonstrates that PNIPAM dehydration, which occurs first at the hydrophobic chain ends, affects the behavior of the entire chains, at least for the Py_n-PNIPAM constructs that were investigated in this study.

ACKNOWLEDGEMENTS

The authors thank NSERC for financial support of this research.

SUPPORTING INFORMATION

Synthetic scheme for the preparation of Py_n-PNIPAM samples, analysis of the fluorescence spectra, comparison between fluorescence spectra and decays, procedure to determine T_c by turbidimetry, tables with FWHM and T_c obtained by two different methods for the turbidimetry measurements.

REFERENCES AND NOTES

1. M. Heskins, J. E. Guillet, *J. Macromol. Sci.: A - Chem.* **1968**, *2*, 1441-1445.
2. A. Halperin, M. Kröger, F. M. Winnik, *Angew. Chem. Int. Ed.* **2015**, *54*, 15342-15367.
3. M. Duan, S. Fang, H. Guo, L. Zhang, *J. Macromol. Sci. B Phys.* **2009**, *48*, 834-843.
4. H. Yang, R. Cheng, Z. A. Wang, *Polymer* **2003**, *44*, 7175-7180.
5. Z. Fang, T. Zhen, *Sci. in China Ser. B* **1998**, *42*, 290-297.
6. N. Ishii, J. Mamiya, T. Ikeda, F. M. Winnik, *Chem. Commun.* **2011**, *47*, 1267-1269.
7. Y. Mylonas, G. Bokias, I. Iliopoulos, G. Staikos, *Eur. Polym. J.* **2006**, *42*, 849-857.

8. X. Qiu, T. Koga, F. Tanaka, F. M. Winnik, *Sci. China Chem.* **2013**, *56*, 56-64.
9. R. Pamies, K. Zhu, A. Kjoniksen, B. Nystrom, *Polym. Bull.* **2009**, *62*, 487-502.
10. P. Kujawa, F. Tanaka, F. M. Winnik, *Macromolecules* **2006**, *39*, 3048-3055.
11. R. Nojima, T. Sato, X. Qiu, F. M. Winnik, *Macromolecules* **2008**, *41*, 292-294.
12. J. Yip, J. Duhamel, X. P. Qiu, F. M. Winnik, *Can. J. Chem.* **2011**, *89*, 163-172.
13. J. Yip, J. Duhamel, X. P. Qiu, F. M. Winnik, *Macromolecules* **2011**, *44*, 5363-5372.
14. C. K. Chee, S. Rimmer, I. Soutar, L. Swanson, *Polymer* **1997**, *38*, 483-486.
15. I. Iliopoulos, J. L. Halary, R. Audebert, *J. Polym. Sci. A* **1988**, *26*, 275-284.
16. T. Koga, F. Tanaka, R. Motokawa, S. Koizumi, F. M. Winnik, *Macromolecules* **2008**, *41*, 9413-9422.
17. F. Tanaka, T. Koga, H. Kojima, F. M. Winnik, *Chin. J. Polym. Sci.* **2011**, *29*, 13-21.
18. T. Koga, F. Tanaka, R. Motokawa, S. Koizumi, F. M. Winnik, *Macromol. Symp.* **2010**, *291-292*, 177-185.
19. F. Tanaka, T. Koga, I. Kaneda, F. M. Winnik, *J. Phys.: Condens. Matter* **2011**, *23*, 284105-284112.
20. H. G. Schild, *Prog. Polym. Sci.* **1992**, *17*, (2), 163-249.
21. F. Afroze, E. Nies, H. Berghmans, *J. Mol. Structure* **2000**, *554*, (1), 55-68.
22. R. G. de Azevedo, L. P. N. Rebelo, A. M. Ramos, J. Szydlowski, H. C. de Sousa, J. Klein, *Fluid Phase Eq.* **2001**, *185*, 189-198.
23. L. P. N. Rebelo, Z. P. Visak, H. C. de Sousa, J. Szydlowski, R. G. de Azevedo, A. M. Ramos, V. Najdanovic-Cisak, M. N. da Ponte, J. Klein, *Macromolecules* **2002**, *35*, 1887-1895.
24. A. Milewska, J. Szydlowski, L. P. N. Rebelo, *J. Polym. Sci. Polym. Phys. Ed.* **2003**, *41*, 1219-1233.
25. Y. Okada, F. Tanaka, *Macromolecules* **2005**, *38*, 4465-4471.
26. P. Kujawa, V. Aseyev, H. Tenhu, F. M. Winnik, *Macromolecules* **2006**, *39*, 7686-7693.
27. P. Kujawa, V. Aseyev, H. Tenhu, F. M. Winnik, *Macromolecules* **2006**, *39*, 7686-7693.
28. S. Fujishige, K. Kubota, I. Ando, *J. Phys. Chem.* **1989**, *93*, 3311-3313.
29. F. Tanaka, T. Koga, F. M. Winnik, *Progr. Colloid Polym. Sci.* **2009**, *136*, 1-8.
30. E. I Tiktopoulo, V. N. Uversky, V. B. Lushchik, S. I. Klenin, V. E. Bychkova, O. B. Ptisyn, *Macromolecules* **1995,** *28,* 7519-7524.
31. Y. Xia, A. D. Burke, H. D. H. Stöver, *Macromolecules* **2006**, *39*, 2275-2283.
32. X. P. Qiu, T. Koga, F. Tanaka, F. M. Winnik, *Sci. China Chem.* **2013**, *56*, 56-64.
33. J. Škvarla, R. K. Raya, M. Uchman, J. Zednik, K. Procházka, V. M. Garamus, A. Meristoudi, S. Pispas, M. Štěpánek, *ASAP Colloid Polym. Sci.* **2017**.
34. Hydrophilic Polymers: Performance with Environmental Acceptability; Glass, J. E.; Ed.; American Chemical Society: Washington, DC, 1996, Vol. 248.
35. Associative Polymers in Aqueous Solution: Glass, J. E., Ed.; American Chemical Society: Washington, DC, 2000, Vol. 765.
36. Z. Li, S. O. Kyerematen, K. Fuchise, R. Kakuchi, R. Sakai, T. Kakuchi, J. Kressler, *Macromol. Chem. Phys.* **2009**, *210*, 2138-2147.
37. L. M. Johnson, Z. Li, A. J. LaBelle, F. S. Bates, T. P. Lodge, M. A. Hillmyer, *Macromolecules* **2017**, *50*, 1102-1112.

38. P. Kujawa, F. Segui, S. Shaban, C. Diab, Y. Okada, F. Tanaka, F. M. Winnik, *Macromolecules* **2006**, *39*, 341-348.
39. F. M. Winnik, *Chem. Rev.* **1993**, *93*, 587-614.
40. W. H. Press, B. P. Flannery, S. A. Teukolsky, W. T. Vetterling, *Numerical Recipes. The Art of Scientific Computing (Fortran Version)*; Cambridge University Press: Cambridge, 1992.
41. J. Duhamel, *Langmuir* **2012**, *28*, 6527-6538.
42. J. Duhamel, *Langmuir* **2014**, *30*, 2307-2324.
43. O. A. Khakhel, *J. Appl. Spec.* **2001**, *68*, 280-286.
44. A. K. Dutta, T. N. A. Misra, *Langmuir* **1996**, *12*, 459-465.

Table of Content

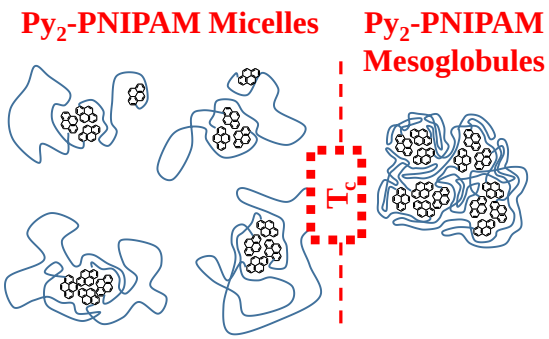

Short text for Table of Content:

"The fluorescence of a series of pyrene-labeled telechelic and semi-telechelic poly(N-isopropylacrylamide) constructs (Py_n-PNIPAM with n = 1 or 2) with a narrow molecular weight distribution was employed to probe the behaviour of the Py_n-PNIPAM samples with temperature as they underwent a coil-to-globule transition (CGT) in water. The fluorescence of pyrene was found to report faithfully on the Py_n-PNIPAM constructs as they underwent their CGT in water."